

ARTICLE

Open Access

Blocking CXCLs–CXCR2 axis in tumor–stromal interactions contributes to survival in a mouse model of pancreatic ductal adenocarcinoma through reduced cell invasion/migration and a shift of immune-inflammatory microenvironment

Makoto Sano^{1,2}, Hideaki Ijichi^{1,3}, Ryota Takahashi¹, Koji Miyabayashi¹, Hiroaki Fujiwara¹, Tomoharu Yamada¹, Hiroyuki Kato¹, Takuma Nakatsuka¹, Yasuo Tanaka¹, Keisuke Tateishi¹, Yasuyuki Morishita⁴, Harold L. Moses⁵, Hiroyuki Isayama^{1,6} and Kazuhiko Koike¹

Abstract

Pancreatic ductal adenocarcinoma (PDAC) is characterized by dense stromal reaction (desmoplasia). We have previously reported that mice with conditional *Kras*^{G12D} mutation and knockout of *TGF-β receptor type II (Tgfr2)*, PKF mice, develop PDAC with desmoplasia modulated by CXC chemokines that are produced by PDAC cells through tumor–stromal interaction. In this study, we further discovered that PDAC and cancer-associated fibroblast (CAF) accelerated each other's invasion and migration through the CXC chemokines-receptor (CXCLs–CXCR2) axis. Heterozygous knockout of *Cxcr2* in PKF mice (PKF2h mice) prolonged survival and inhibited both tumor angiogenesis and PDAC microinvasion. Infiltration of neutrophils, myeloid-derived suppressor cells (MDSCs), and arginase-1⁺ M2-like tumor-associated macrophages (TAMs) significantly decreased in the tumors of PKF2h mice, whereas inducible nitric oxide synthase (iNOS)⁺ M1-like TAMs and apoptotic tumor cells markedly increased, which indicated that blockade of the CXCLs–CXCR2 axis resulted in a shift of immune-inflammatory microenvironment. These results suggest that blocking of the CXCLs–CXCR2 axis in tumor–stromal interactions could be a therapeutic approach against PDAC progression.

Introduction

Pancreatic ductal adenocarcinoma (PDAC), a usually lethal and common type of pancreatic cancer, is the third and fourth leading cause of cancer death in the United

States¹ and Japan². Five-year survival rate is still around 8%, partially attributed to the difficulty of early diagnosis, while postsurgical 5-year survival is still around 20%. The poor prognosis of PDAC is due to aggressive malignant potentials including invasive and metastatic activity^{3,4}.

Progression of the PDAC is thought to result in the accumulation of specific genetic alterations through pre-malignant pancreatic intraepithelial neoplasia (PanIN) and the invasive stage⁵. An activating point mutation of the *KRAS* proto-oncogene is observed in more than 95%

Correspondence: Hideaki Ijichi (hideijichi-gi@umin.ac.jp)

¹Department of Gastroenterology, Graduate School of Medicine, The University of Tokyo, 7-3-1 Hongo, Bunkyo-ku, Tokyo 113-8655, Japan

²Division of Human Pathology, Department of Pathology and Microbiology, Nihon University School of Medicine, 30-1 Oyaguchikamicho, Itabashi-ku, Tokyo 173-8610, Japan

Full list of author information is available at the end of the article.

© The Author(s) 2019



Open Access This article is licensed under a Creative Commons Attribution 4.0 International License, which permits use, sharing, adaptation, distribution and reproduction in any medium or format, as long as you give appropriate credit to the original author(s) and the source, provide a link to the Creative Commons license, and indicate if changes were made. The images or other third party material in this article are included in the article's Creative Commons license, unless indicated otherwise in a credit line to the material. If material is not included in the article's Creative Commons license and your intended use is not permitted by statutory regulation or exceeds the permitted use, you will need to obtain permission directly from the copyright holder. To view a copy of this license, visit <http://creativecommons.org/licenses/by/4.0/>.

of PDAC cases, whereas inactivation of tumor suppressor genes, including *CDKN2A*, *TP53*, and *SMAD4/DPC4*, have been shown to increase in frequency with progression of PanIN to PDAC⁶. Meanwhile, mutation of *TGFBR2* (*TGF- β receptor type II*), a tumor suppressor gene, is less frequently detected in lesions in PanIN/PDAC compared with *SMAD4/DPC4*⁷, both of which function in the TGF- β -SMAD signaling pathway. However, decrease of *TGFBR2* expression is observed in nearly half of the PDAC cases^{8,9}, indicating that inactivation of TGF- β -SMAD signaling is important in PanINs/PDAC progression.

We previously reported a genetically engineered mouse model with pancreas epithelium-specific activation of *Kras*^{G12D} and knockout of *Tgfr2* (*Ptfla*^{cre/+}; *LSL-Kras*^{G12D/+}; *Tgfr2*^{flox/flox}) (called PKF mice), which develops PDAC with abundant stromal reaction (desmoplasia)^{10,11}. Indeed, we found that PDAC cells in PKF mice secrete several CXC chemokines (Cxcl 1, 2, 5, and 16) into the tumor stroma and promote desmoplastic reactions and tumor angiogenesis. Inhibition of CXC chemokine receptor type 2 (CXCR2), a G-protein-coupled receptor, blocked the tumor angiogenesis via downregulation of connective tissue growth factor (Ctgf) expression in the tumor-associated fibroblasts (TAFs), leading to an anti-tumor effect and significant survival extension¹¹. However, TAFs used in the study were derived from mPanIN tissues and a whole image of the stromal response to the tumor other than Ctgf upregulation in TAFs still remains unclear.

CXC chemokines and CXCR2 were originally considered to contribute to neutrophil chemotaxis in response to tissue injury and infections^{12–15}. Recent studies indicated that infiltration of neutrophils and myeloid-derived suppressor cells (MDSCs) through the CXC ligands (CXCLs)–CXCR2 signaling also contribute to tumor progression in various cancers including PDAC^{16,17}. Indeed, mice with global knockout of *Cxcr2* demonstrated significant reduction of MPO⁺ neutrophils and Cd11b⁺Ly-6G⁺ MDSCs in *Kras*^{G12D}-induced PDAC¹⁸. In addition, the CXCLs–CXCR2 axis can also promote angiogenesis directly through endothelial proliferation and vascular tube formation^{19,20}. Thus, the CXCLs–CXCR2 axis is highly involved in PDAC progression, especially in tumor–stromal interactions and the tumor microenvironment.

In the present study, we separated cancer-associated fibroblasts (CAFs) from PKF PDAC tissues and demonstrated upregulation of CXCR2 ligands in the CAFs stimulated by conditioned media of the PDAC cells. In addition, we found that the CXCLs–CXCR2 axis plays important roles in migration or invasion of PDAC cells as well as CAFs *in vitro* and *in vivo*. Moreover, we demonstrated that blocking of CXCLs–CXCR2 axis *in vivo*

induces tumor cell apoptosis with a shift of infiltrated immune-inflammatory cells in the PDAC lesions, as evidenced by reduced infiltration of neutrophils/MDSCs and arginase-1-positive macrophages, and increased inducible nitric oxide synthase (iNOS)-positive macrophages, leading to significant survival extension of PDAC-bearing mice. Thus, CXCLs–CXCR2 axis could be one of the potent therapeutic targets for PDAC.

Results

PDAC cells and CAFs mutually promote invasion/migration by activating the CXCLs–CXCR2 axis

In this study, we analyzed in detail the response of CAFs to PDAC cells in the tumor–stromal interaction. Characterization of PDAC cells and CAFs was previously reported¹¹, whereas additional CAFs obtained from the PDAC tissues of PKF mice were validated. No recombination of the *LSL-Kras*^{G12D} and *Tgfr2*^{flox} alleles in the CAFs was detected by polymerase chain reaction (PCR), since the recombination was driven by pancreas epithelium-specific *Ptfla*^{Cre}. Almost all the CAFs were spindle shaped and double positive for the expression of α -smooth muscle actin (α -SMA) and fibroblast specific protein 1 (FSP1) (Supplementary Fig. 1). Changes in the gene expression profile in the CAFs after stimulation with conditioned media (CM) of PDAC cells was analyzed using gene-expression microarray, which identified 580 upregulated genes with an adjusted *P* value of 0.05 and greater than twofold change in expression between the groups. Of the 580 genes, major genes are shown in Fig. 1a, Supplementary Fig. 2 and Supplementary Table 1. Interestingly, *Cxc* chemokines including *Cxcl1*, *Cxcl2*, and *Cxcl3*, which are ligands of CXCR2, were upregulated in CAFs after stimulation by PDAC–CM (Fig. 1a). In addition, the stimulated CAFs synthesized other chemokines such as *Ccl2*, *Ccl3*, *Ccl6*, *Ccl7*, *Ccl9*, and *Ccl20*, as well as the inflammatory cytokines *IL-1 β* , *IL-1 β* , and *TNF* (Supplementary Fig. 2 and Supplementary Table 1). Meanwhile, upregulation of *Cxcl1*, *Cxcl2*, and *Cxcl3* in CAFs treated with PDAC–CM was confirmed by quantitative reverse transcription PCR (qRT-PCR) (Fig. 1b and Supplementary Fig. 3). These results indicate that the CAFs produce the same CXCLs that PDAC cells are secreting as a response to stimuli from PDAC cells in the tumor–stromal interaction.

Next, we performed transwell invasion/migration assays to examine the effect of tumor–stromal interactions on the PDAC cells and CAFs. The invasion of PDAC cells was significantly enhanced by addition of CAF–CM (Fig. 1c), whereas the invasion activity was reduced in a dose-dependent manner by CXCR2-specific inhibitor SB225002 (Fig. 1c). Interestingly, migration activity of CAFs was increased by mPanIN cell–CM and was further enhanced by PDAC cell–CM compared with that with

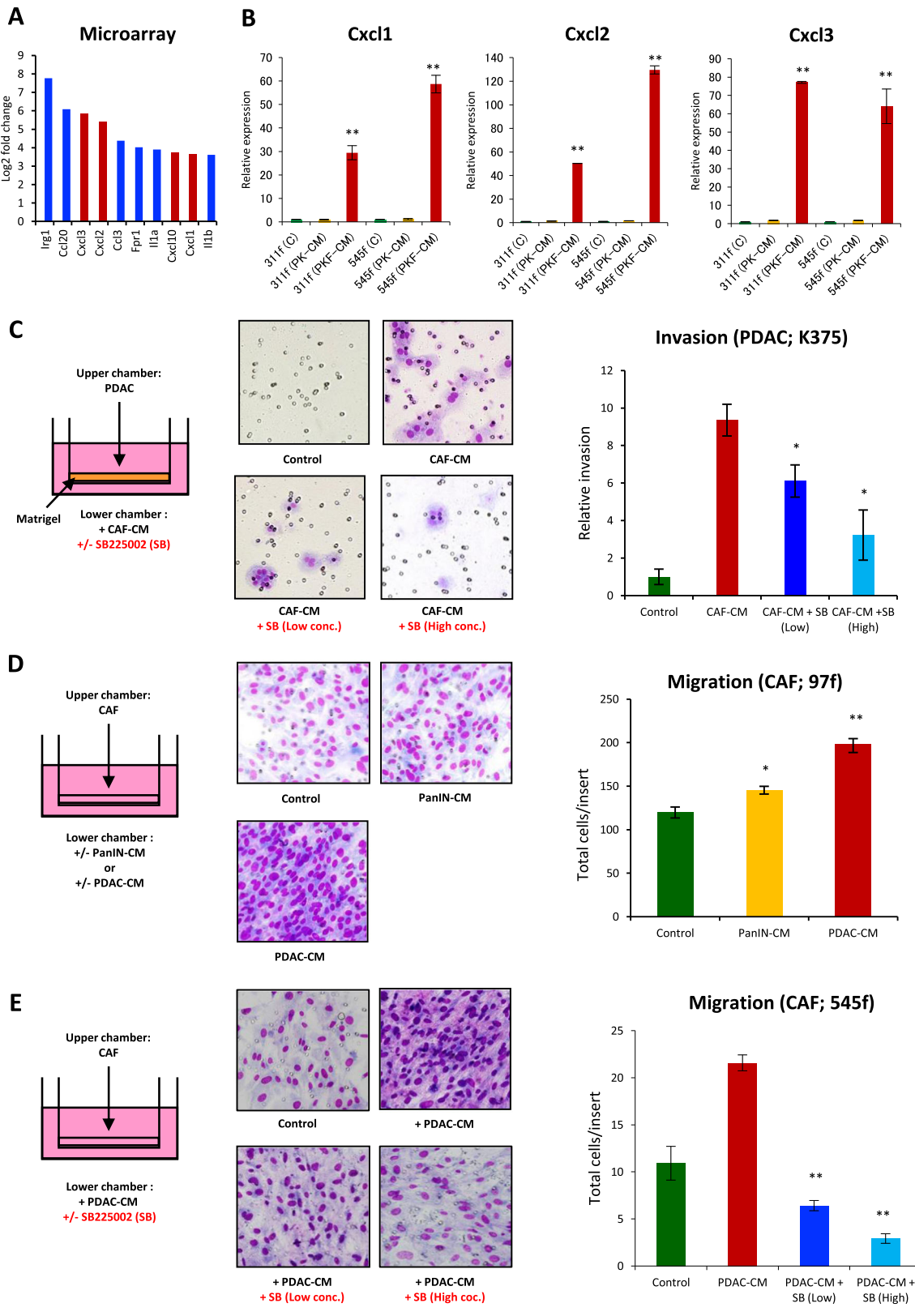


Fig. 1 (See legend on next page.)

(see figure on previous page)

Fig. 1 Interactions of PDAC cells and cancer-associated fibroblasts (CAFs) mediated by CXCLs–CXCR2 signaling pathway. **a** Top 10 upregulated genes in CAFs after stimulation with conditioned medium (CM) of PDAC cell lines derived from PKF (*Ptfl1a^{cre/+};LSL-Kras^{G12D/+};Tgfb2^{flox/flox};Cxcr2^{+/-}*) mice in the microarray analysis. *Cxcl* genes are red-colored. **b** qRT-PCR analysis in CAFs (311f, 545f) after addition of CM from mPanIN cells (PK-CM) or PDAC cells (PKF-CM). Data are means \pm standard error (SE). $^{**}p < 0.01$ compared to the control (C) and (PK-CM). **c** Invasive activity of PDAC with CM of CAFs with/without CXCR2 inhibitor SB225002. Data are means \pm SE. $^{*}p < 0.05$ compared to the CAF-CM. **d** Migration of CAFs with CM of mPanIN or PDAC. Data are means \pm SE. $^{*}p < 0.05$, $^{**}p < 0.01$ compared to the control. **e** Inhibition of CAF migration by CXCR2 inhibitor SB225002. Data are means \pm SE. $^{**}p < 0.01$ compared to the PDAC-CM

mPanIN–CM (Fig. 1d). The migration of CAFs was also decreased by CXCR2 inhibitor SB225002 in a dose-dependent manner (Fig. 1e). Meanwhile, proliferative activity of PDAC cells and CAFs was not affected by CXCR2 inhibitor (Supplementary Fig. 4). These results suggest that PDAC cells promote the migration of CAFs, and in turn, CAFs activate the invasion of PDAC cells, both by secreting the same CXCLs into the tumor microenvironment and activating the CXCLs–CXCR2 axis, without directly affecting cell proliferation. This bidirectional chemokine signaling might be highly involved in the invasion and metastasis of PDAC, which might explain the underlying mechanisms of the extended survival of PDAC-bearing mice with CXCR2 inhibitor treatment, which we have previously reported¹¹.

Heterozygous knockout of *Cxcr2* significantly extend the survival of PDAC mice, which is associated with inhibition of microvessel invasion

These results suggested importance of the CXCLs–CXCR2 axis in PDAC progression and prompted us to knock out *Cxcr2* in the PKF mice (*Ptfl1a^{cre/+};LSL-Kras^{G12D/+};Tgfb2^{flox/flox};Cxcr2^{-/-}*) to investigate whether we could dramatically prevent PDAC formation or progression. However, progeny of homozygous *Cxcr2* knockout could not be obtained. Although homozygous *Cxcr2* knockout was achieved in other PDAC models¹⁸, it might be due to the different *Cxcr2^{-/-}* mouse strain used. Thus, we used heterozygous knockout of *Cxcr2* in the context of PKF (*Ptfl1a^{cre/+};LSL-Kras^{G12D/+};Tgfb2^{flox/flox};Cxcr2^{+/-}*) (PKF2h). Even with the heterozygous knockout of *Cxcr2*, survival of PKF2h mice was significantly extended compared to that of PKF mice based on Kaplan–Meier analysis (median survival 75 days vs. 56 days, $p = 0.0164$) (Fig. 2a). Gender bias was not detected in the survival ratio, both in the PKF and PKF2h mice.

However, heterozygous knockout of *Cxcr2* did not prevent PDAC formation, and there was no significant difference in gross appearance of pancreatic tumor as well as tumor weight between PKF and PKF2h mice (Fig. 2b, c). Indeed, no statistical difference of histological status, including premalignant mPanINs and PDAC, was found between PKF and PKF2h mice (Fig. 2d, e). The observed

number of Ki-67-positive proliferating cells was similar in the tumor/juxtatumoral stroma and desmoplastic stroma (Fig. 2d, f), also indicating that heterozygous knockout of *Cxcr2* in vivo was not directly correlated to proliferation of PDAC.

Next, we performed staining for CD31 and LYVE-1 to study tumor invasion into the vein and lymph vessels, respectively (Fig. 2g), because invasion of PDAC cells was inhibited by CXCR2 inhibitor in vitro. Similar to the invasion assay, PDAC microinvasion into CD31⁺ tumor blood vessels was significantly reduced in PKF2h mice (3/6; 50%) compared to PKF mice (7/7; 100%). In addition, microinvasion into LYVE-1⁺ lymph vessels was decreased in PKF2h mice (3/6; 50%) compared to PKF mice (5/7; 71.4%). Interestingly, CD31⁺ tumor microvessel density significantly decreased in both the pancreatic juxtatumoral and desmoplastic stroma of PKF2h mice (Fig. 2d, f). Therefore, it is considered that heterozygous knockout of *Cxcr2* in PDAC cells, CAFs and endothelial cells, in which CXCR2 activation by PDAC–CAF interactions is interrupted, leads to inhibition of PDAC vessel invasion. Meanwhile, heterozygous *Cxcr2* knockout in endothelial cells of blood vessels may block tumor angiogenesis during the PDAC progression in PKF2h mice.

Antitumor effect is induced by increase of antitumor iNOS⁺ macrophages in heterozygous *Cxcr2* knockout PDAC mice

In other *Cxcr2*-knockout mouse models, significant decrease of neutrophil infiltration into the local area including dermatitis and PDAC has been reported^{18,21,22}. We thus investigated inflammatory cell infiltration in the pancreatic tumor of PKF and PKF2h mice. Similar to the previous reports, decrease of myeloperoxidase⁺ (MPO⁺) neutrophil infiltration was observed in the pancreatic tumor area in PKF2h mice (Fig. 3a, b). We performed double staining with CD11b and Ly-6G, because infiltration of MDSCs is known to be important in PDAC progression²³, and observed that CD11b⁺Ly-6G⁺ MDSCs significantly decreased in the tumor of PKF2h mice (Fig. 3a, b).

Numerous F4/80⁺ macrophages also infiltrated in the tumor stroma with dense desmoplastic reaction in both

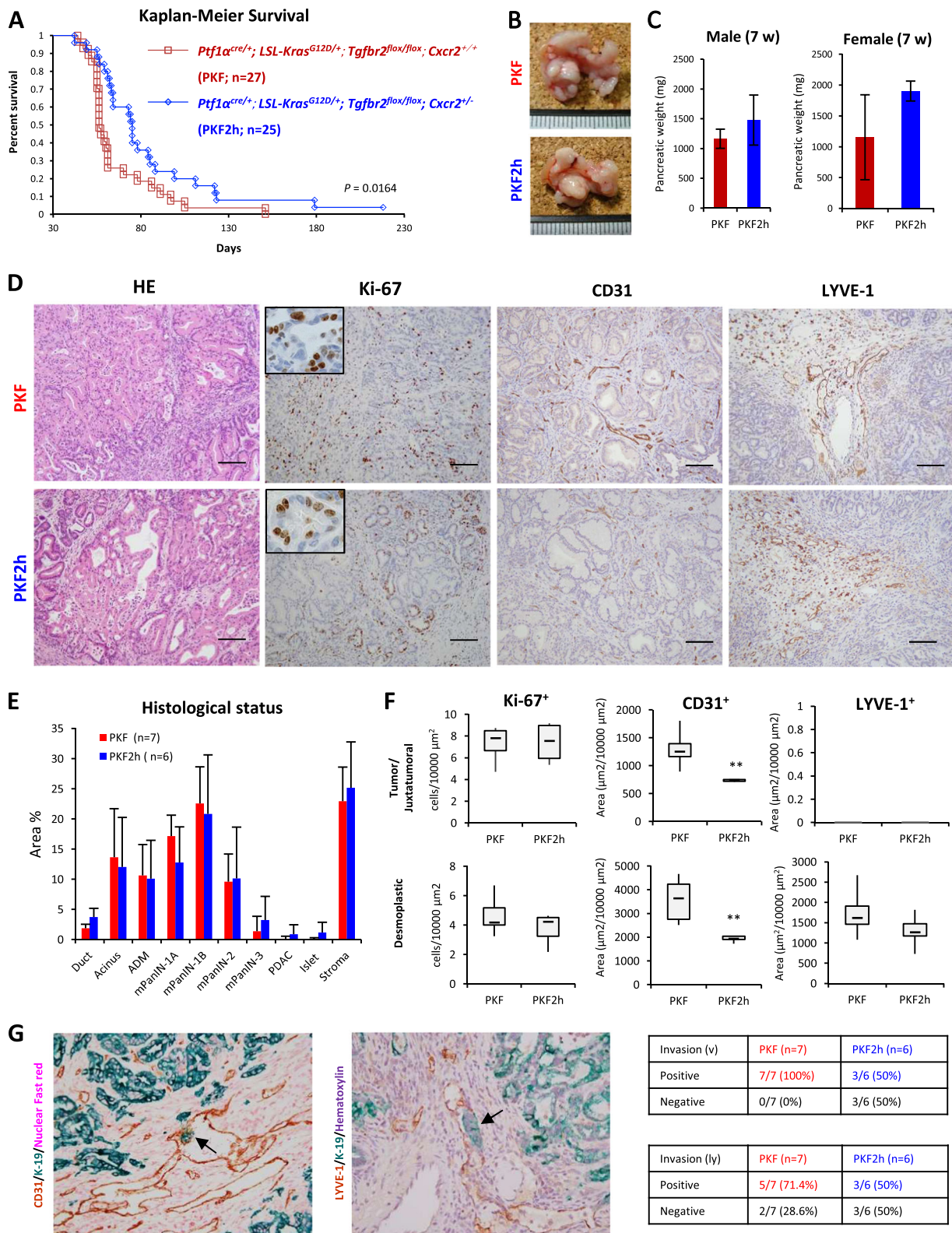
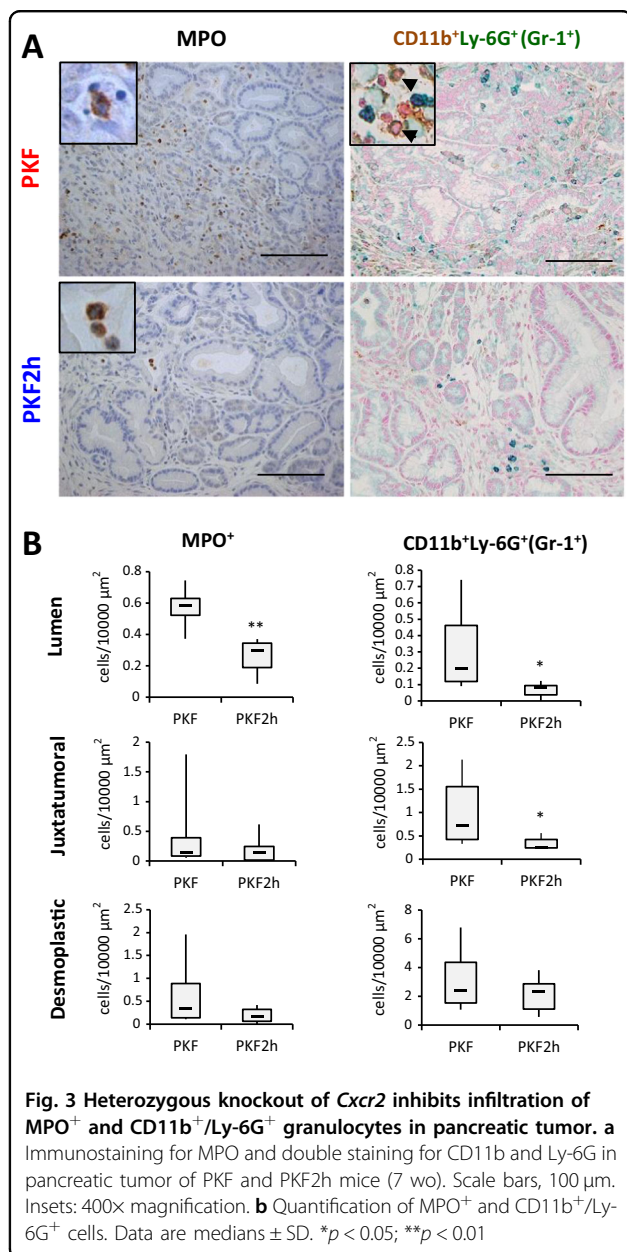


Fig. 2 (See legend on next page.)

(see figure on previous page)

Fig. 2 Heterozygous knockout of *Cxcr2* is associated with better outcome of PDAC mice with inhibition of PDAC vessel invasion. a Kaplan–Meier survival analysis of PKF ($n = 27$) and PKF2h ($n = 25$; *Ptfl1*^{cre/+};*LSL-Kras*^{G12D/+};*Tgfbir2*^{fllox/fllox};*Cxcr2*^{hetero+/-}) mice. $P = 0.0164$ by log-rank test. **b** Gross appearance of pancreatic tumor in PKF and PKF2h mice (7 weeks old (wo)). **c** Pancreatic tumor weight (7 wo). Data are medians \pm standard deviation (SD). **d** Histopathological findings including staining for Ki67, CD31, and LYVE-1 in pancreatic tumor in 7-wo PKF ($n = 7$) and PKF2h mice ($n = 6$). Scale bars, 100 μ m. Insets: 400 \times magnification. **e** Histogram of histopathological status of the pancreatic tumor (7 wo). ADM acinar ductal metaplasia. **f** Count of stained cells in the tumor ductal lumen, juxtatumoral, or dense interlobular stroma with desmoplastic reaction (desmoplastic stroma). Data are medians \pm SD. * $p < 0.05$; ** $p < 0.01$. **g** Microscopic invasion of PDAC (arrows) into veins or lymph vessels analyzed by double staining with epithelial marker K-19 and CD31 or LYVE-1

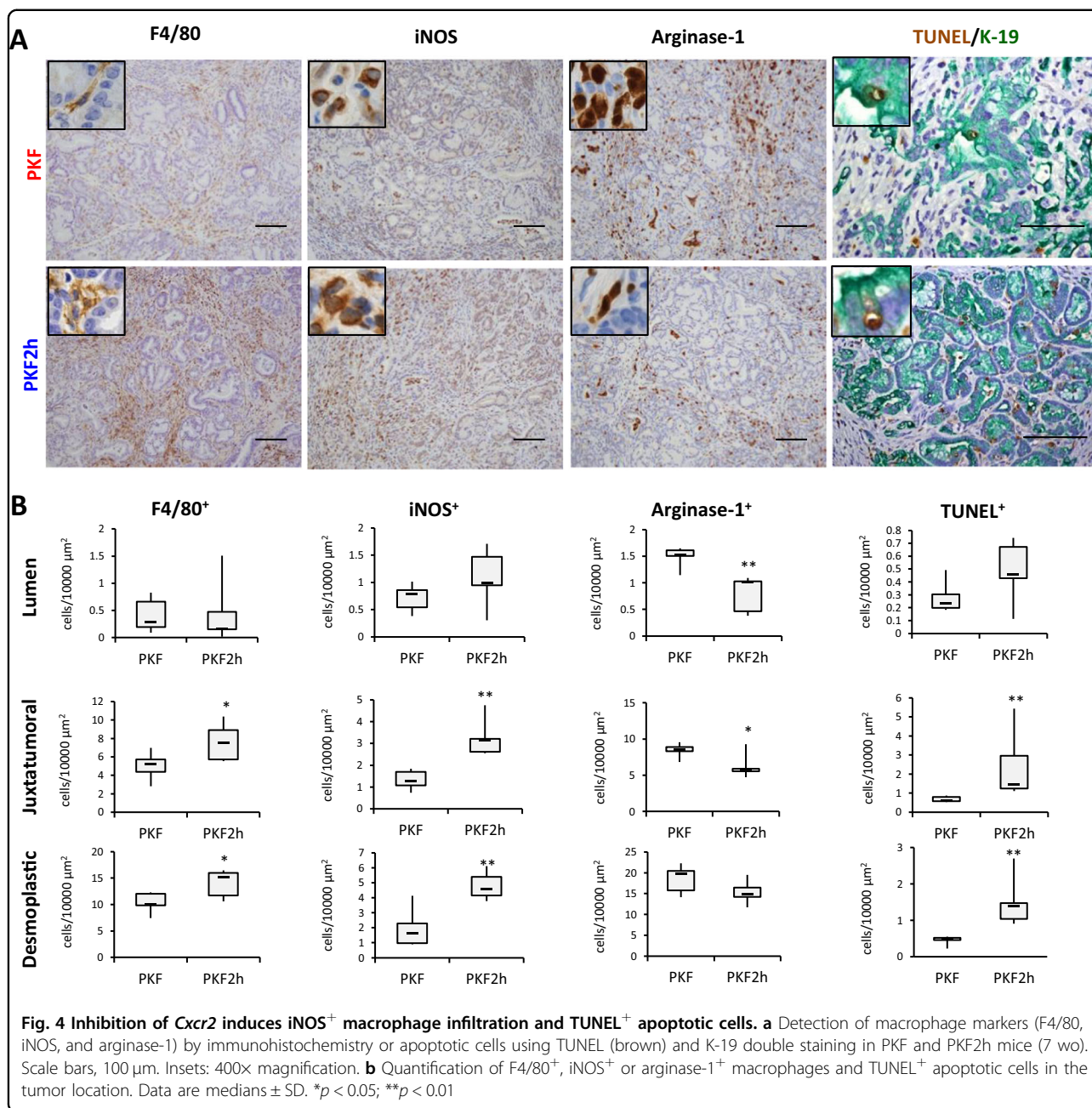


PKF and PKF2h mice (Fig. 4a, b). Inflammatory macrophages can be classified into two types: pro-inflammatory M1 and anti-inflammatory M2 macrophages²⁴. M1 macrophages express iNOS, which metabolizes arginine to NO and plays a role in antitumor effect, whereas M2 macrophages express arginase, which hydrolyzes arginine to ornithine and urea, and has anti-inflammatory and tissue repair effects²⁴. Thus, we next performed staining for iNOS and arginase-1 to functionally determine the phenotype of infiltrated macrophages as M1 or M2. Interestingly, iNOS⁺ M1-like macrophages significantly increased in the tumor stroma of PKF2h mice, whereas arginase-1⁺ M2-like macrophages tended to decrease (Fig. 4a, b). TUNEL⁺ apoptotic cells significantly increased in PKF2h mice (Fig. 4a, b), which was consistent with the previous report that classical iNOS⁺ M1-like tumor-associated macrophages (TAMs) possess anti-tumor effects by secreting cytoplasmic NO and inducing apoptosis²⁵. In the TUNEL/K-19 double staining, we observed that TUNEL⁺ cells in the juxtatumoral area were also K-19⁺ tumor cells (Fig. 4a), which indicated that apoptotic tumor cells increased in PKF2h compared with PKF mice. We also observed that TUNEL⁺/K-19⁻ apoptotic stromal cells increased in the desmoplastic area in PKF2h mice.

Infiltration of lymphocytes was also analyzed in PKF and PKF2h mice, which revealed that infiltration of cytotoxic CD8⁺ T cells and regulatory T cell-specific FoxP3⁺ cells decreased in the pancreatic tumor nest in PKF2h mice, whereas no significant difference of CD4⁺ suppressor T cells and CD45R⁺ B lymphocytes was detected between PKF and PKF2h mice (Fig. 5a, b). These results suggest that infiltration of iNOS⁺ M1-like TAMs, but not cytotoxic CD8⁺ lymphocytes, could have an important role in the anti-tumor effect on PDAC in PKF2h mice. Reduced infiltration of MPO⁺ neutrophils and MDSCs might also be involved in the inhibited PDAC progression in PKF2h mice.

Discussion

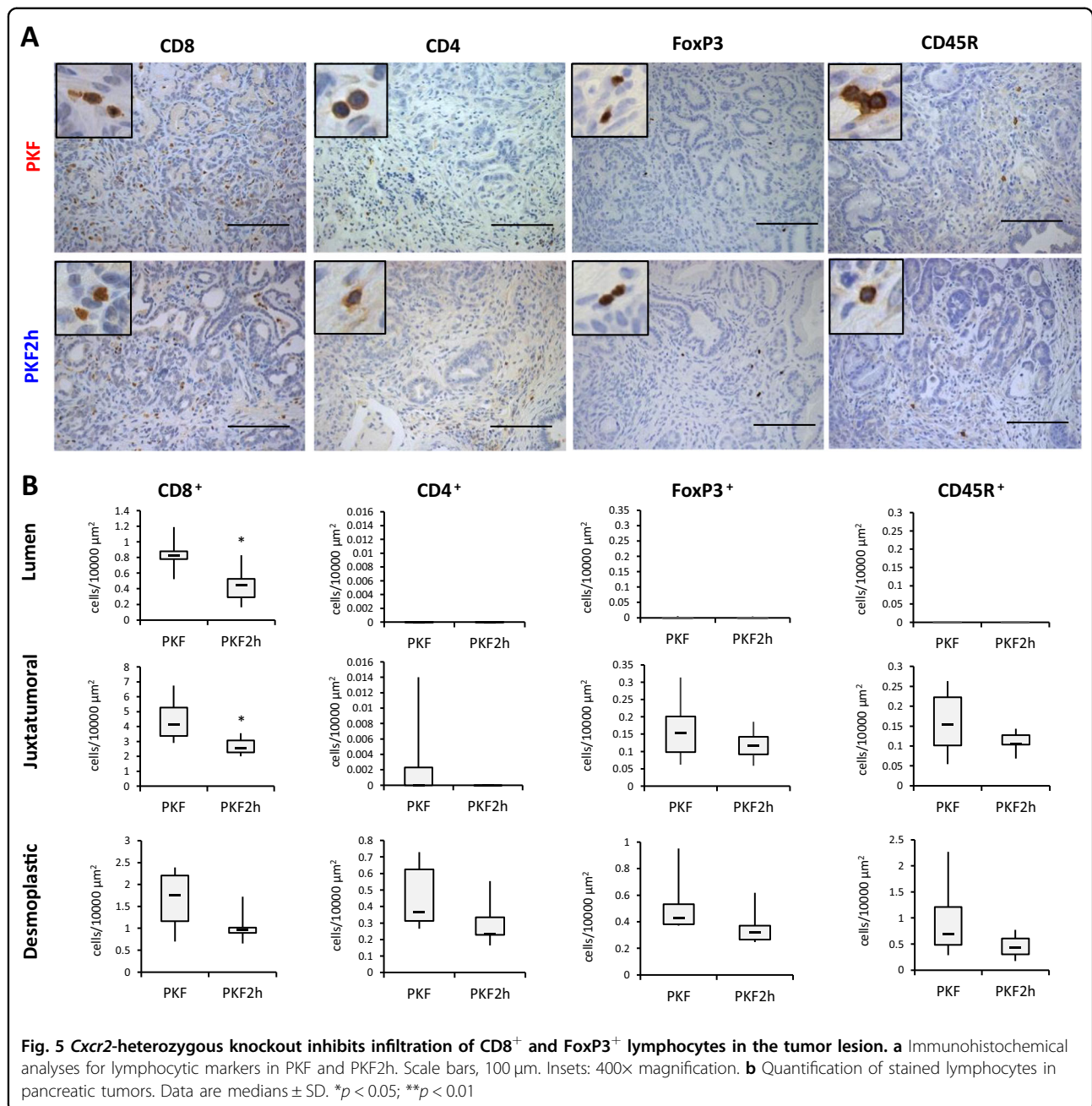
In this study, we explored stromal–tumor interactions in PDAC to elucidate how CAFs respond to the tumor cells. By screening upregulated factors in mouse CAFs after stimulation with PDAC cell conditioned medium, we



determined that *Cxcl1–3* were upregulated in CAFs, some of which were also highly produced by PKF-derived PDAC cells¹¹. In human PDAC, expression of *CXCL1* and *-5* is upregulated compared with that in normal pancreatic duct, whereas high levels of *CXCL1*, *-5*, and *-8* are significantly detected in the pancreatic fluid of PDAC patients^{19,26}, which may also be partially derived from CAFs. Previously, we focused on *Ctgf*, which was induced in mPanIN-derived TAFs by PDAC stimuli¹¹; however, we found in this study that upregulation of the *Cxcls* was much higher than that of *Ctgf* in the CAFs derived from the PDAC. In addition, this study revealed that the

activated *CXCLs–CXCR2* axis promoted invasion of PDAC cells and migration of CAFs. The PDAC cells and CAFs might attract each other by secreting the *CXCLs* and invade together; this may contribute to the PDAC invasion and desmoplasia formation, and might support the idea that invasion and metastasis of PDAC cells are accompanied and/or directed by CAFs²⁷. A scheme of suggested tumor-promoting tumor–stromal interactions is shown in Fig. 6a.

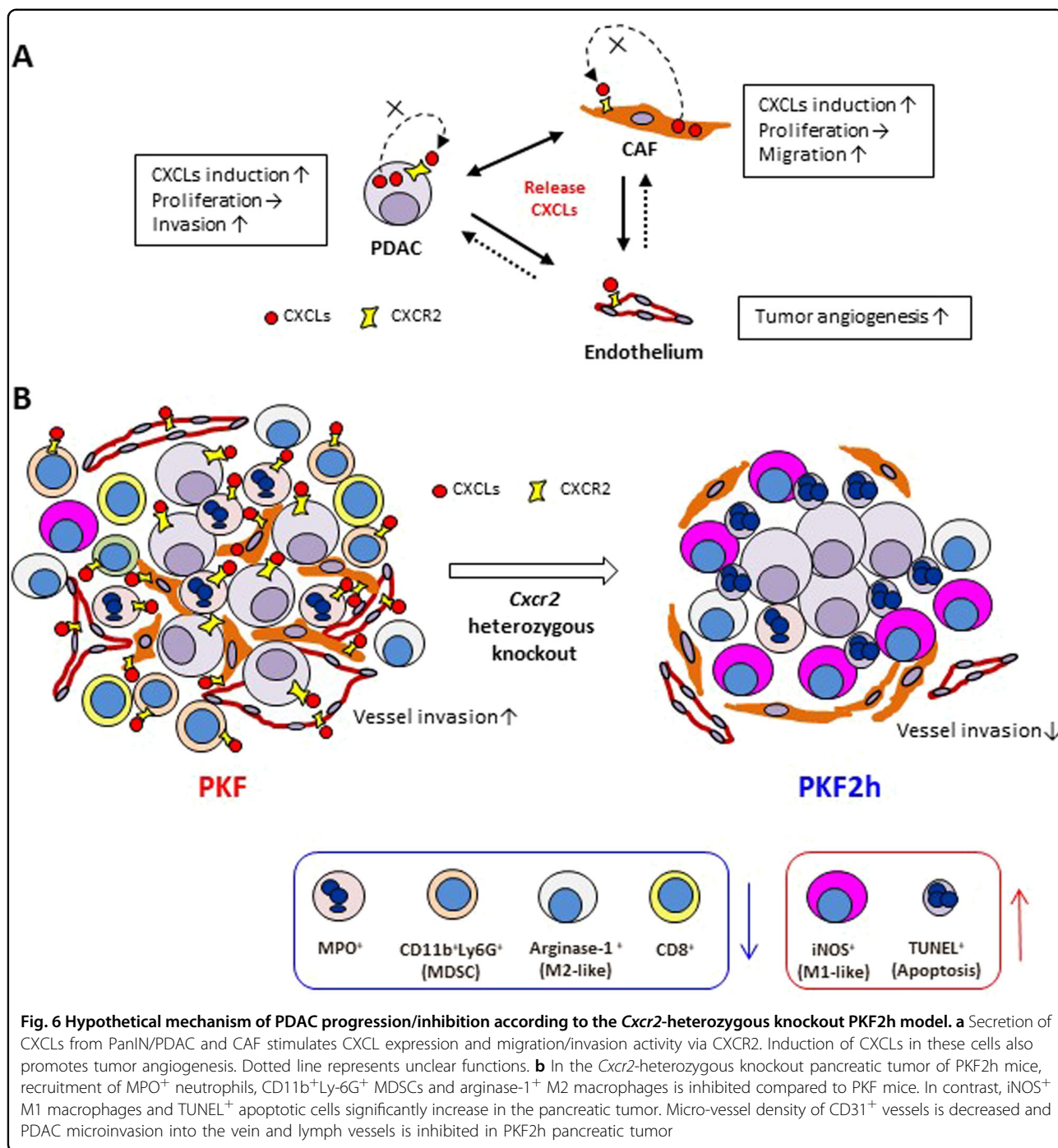
This study suggests that heterozygous *Cxcr2* knockout causes a shift of immune–inflammatory tumor microenvironment as shown in Fig. 6b. In the heterozygous



Cxcr2 knockout PKF2h mice, MPO⁺ neutrophils and CD11b⁺Ly-6G⁺ MDSCs significantly decreased in the tumor nest. Another study also showed significant reduction of neutrophil and MDSC infiltration in the PDAC mice with global knockout of *Cxcr2*¹⁸. In contrast, pancreas epithelial-specific loss of *Cxcr2* induced recruitment of neutrophils and MDSCs into the tumor nest and enhanced PDAC metastasis¹⁸. Therefore, the *Cxcr2* knockout in the stromal components of PDAC is contributing to the inhibition of neutrophil and MDSC

recruitment, which might be one of the antitumor mechanisms.

Infiltration of F4/80⁺ macrophages is closely related to *Kras*^{G12D}-induced acinar ductal metaplasia, mPanIN and PDAC development²⁸. In an experimental inflammatory model in *Cxcr2*-null mice, marked reduction of neutrophil infiltration was observed in the cutaneous inflammation, while Mac2⁺ macrophages significantly increased²². Likewise, in contrast to neutrophils, F4/80⁺ TAMs significantly infiltrated into the tumor lesions in our *Cxcr2*-



heterozygous knockout mice as well as in the other PDAC model with *Cxcr2*-knockout¹⁸. In general, macrophages infiltrate at the chronic inflammatory stage after acute inflammation with neutrophil infiltration. Thus, neutrophil reduction could induce F4/80⁺ TAM infiltration in the tumor nest in an innate manner. Presence of TAMs has been recognized as a poor prognostic marker in cancers including PDAC²⁹. TAMs enhance invasion/metastasis and neovascularization of PDAC and inhibit

the adaptive tumor-specific immune response by secreting proteases, chemokines and angiogenic factors²⁹. In particular, M2-like TAMs are increased in the tumor lesion and associated with tumor progression and poor prognosis²⁹. We further evaluated the functional markers of macrophages and found that infiltration of arginase-1⁺ M2-like TAMs decreased in the mPanIN/PDAC lesions, whereas iNOS⁺ M1-like TAMs increased in the tumor area, resulting in a significant induction of apoptosis of

the tumor cells (Fig. 6b). M2-like TAMs are recently known to be transformed into M1 macrophages in pathological environments^{30,31}. Although the detailed mechanism behind decreased M2-like TAMs and increased M1-like TAMs in PKF2h mice remains to be elucidated, increase of M1/M2 ratio by *Cxcr2* inhibition would be effective for modulating the immune tumor microenvironment of PDAC.

In contrast with the neutrophil, MDSC and macrophage infiltration, the impact of infiltrated lymphocytes appeared to be small in this study. Another group reported that CD3⁺ T cell infiltration increased in the pancreatic tumor nest in PDAC mice with global knockout of *Cxcr2*¹⁸. In addition, cytotoxic subpopulations of CD8⁺ T cells were not described and the increased CD3⁺ T cells did not prolong the survival of *Cxcr2* knockout mice significantly; however, cytotoxic activity of the CD3⁺ T cells was suggested after treatment with programmed cell death protein 1 (PD-1) antibody. In our model, tumor-infiltrated cytotoxic CD8⁺ T cells decreased in heterozygous *Cxcr2* knockout PKF2h mice. Even in PKF mice with *Cxcr2*-wild type, only a few CD8⁺ T cells were observed in the tumor lesions. The number of infiltrated CD4⁺ helper T cells, FoxP3⁺ regulatory T cells, and CD45R⁺ B lymphocytes was also small in the tumor lesions of PKF and PKF2h mice.

In this study, heterozygous knockout of *Cxcr2* significantly extended the survival of PDAC mice. Recent studies demonstrated that treatment with CXCR2 inhibitor prolonged the survival of two different PDAC models, *Kras*^{G12D} + *Tgfb2* knockout (PKF) and *Kras*^{G12D} + Tp53 inactivation (KPC)^{11,18}, which is consistent with this study. However, global homozygous knockout of *Cxcr2* in the KPC mice did not extend the survival¹⁸. Thus, progression of PDAC with *Kras*^{G12D} + *Tgfb2* knockout might be more dependent on the CXCLs–CXCR2 axis than the PDAC with *Kras*^{G12D} + Tp53 inactivation. Our previous observation and current study suggested some of the underlying mechanisms in the *Kras*^{G12D} + *Tgfb2* knockout: the Cxc chemokines expression in the pancreatic epithelial cells was highly correlated with TGF- β signaling, upregulated in the *Tgfb2*-knockout cells and downregulated by adding TGF- β in the *Tgfb2*-intact cells¹¹, the Cxcls expression in the CAFs was induced by the PDAC cells, PDAC cell invasion and CAF migration were induced by each other in a *Cxcr2*-dependent manner. Although further investigations are necessary to elucidate the detailed mechanisms of the CXCLs–CXCR2 axis dependency of PDAC progression, blocking CXCLs–CXCR2 axis in the cross-talk between tumor and stromal cells could be a promising therapeutic strategy for PDAC.

Materials and methods

Cell lines and reagent

Establishment and characterization of cell lines including *Ptf1a*^{cre/+}; *LSL-Kras*^{G12D/+}; *Tgfb2*^{flox/flox} mouse (PKF)-derived pancreatic ductal adenocarcinoma (PDAC; K375 and K399), *Ptf1a*^{cre/+}; *LSL-Kras*^{G12D/+} mouse (PK)-derived mPanIN tissues (K512 and K518) and cancer-associated fibroblast (CAF; 97f) have been described^{10,11,32}. CAFs (311f, 545f) were also established from primary PDAC sites in PKF mice and were validated by recombination PCR of *LSL-Kras*^{G12D} and *Tgfb2*^{flox} alleles¹⁰ and immunofluorescence with α -SMA and FSP1 (Supplementary Fig 1). CXCR2 inhibitor SB225002 was obtained from Calbiochem.

Gene-expression profiling microarray

After stimulation by conditioned medium of mixed PDAC cell lines (K375 and K399), RNAs of mixed CAF cell lines (97f, 311f, and 545f) were extracted using Nucleospin RNA II kit (TaKaRa) and treated with RQ1 DNase (Promega), then the RNA samples were labeled using the 3' IVT Express Kit (Affymetrix, 901,228) and subjected to gene expression profiling using GeneChip Mouse Genome 430 2.0 arrays (Affymetrix, 900,495). Raw data is available in Figshare repository (<https://figshare.com>).

qRT-PCR

cDNA was generated from 0.5 μ g of total RNA using ImProm-II Reverse Transcription system (Promega). qRT-PCR was performed using FastStart Universal SYBR Green Mastermix (Roche) and StepOnePlus realtime PCR system (Applied Biosystems) according to the manufacturers' instructions. The amount of PCR product was normalized against GAPDH as an internal control. Experiments were repeated twice in duplicate.

Primer pairs used are shown in Supplementary Table 2.

Matrigel invasion assay

Matrigel invasion assay was performed using BD Bio-Coat Matrigel Invasion Chamber (BD Biosciences). PDAC cells (5×10^4) were plated into Matrigel-coated invasion chamber inserts and incubated with 20% FBS-containing culture media for 48 h, with or without CAF-derived conditioned media in the lower chamber. The invaded cells were counted using Diff-Quick stain (Sysmex) as described previously³³. To determine the effect of CXCLs–CXCR2 axis, 0.4 or 4 μ M SB225002 or DMSO (control) was added into the lower chamber containing CAF-derived conditioned media. Experiments were repeated three times in triplicate.

Migration assay

CAFs (2×10^5) were plated into the upper chamber inserts (BD Biosciences) and incubated with 20% FBS-contained culture media for 24 h, with or without mPanIN- or PDAC-derived conditioned media in the lower chamber. The migrated cells were counted using Diff-Quick stain. To determine the effect of CXCLs–CXCR2 axis, 0.4 or 4 μ M SB225002 or DMSO (control) was added into the lower chamber containing PDAC-derived conditioned media. Experiments were repeated three times in triplicate.

Mice

Generation of *Ptfla*^{cre/+};*LSL-Kras*^{G12D/+};*Tgfr2*^{flox/flox}; *Cxcr2*^{+/+} (PKF) mice and the genotyping have been described previously^{10,11}. *Ptfla*^{cre/+};*LSL-Kras*^{G12D/+};*Tgfr2*^{flox/flox}; *Cxcr2*^{+/-} (PKF2h) mice were generated by crossing PKF mice with *Cxcr2*^{+/-} mice obtained from Jackson Laboratories³⁴. Background of all the mice used in this study was C57BL/6, after repeated backcrossing. All animals were kept in specific pathogen-free housing with abundant food and water under guidelines approved by the ethics committee for the Care and Use of Laboratory Animals of the University of Tokyo.

Histology and immunohistochemistry (IHC)

All murine samples were fixed in 4% paraformaldehyde and embedded in paraffin, as described previously^{10,11}. Three-micrometre sections were stained with hematoxylin & eosin (HE) and mPanIN/PDAC status were analyzed as described previously³⁵. Antibodies used for IHC staining are summarized in Supplementary Table 3. The staining was performed as described previously^{11,35}. DAB substrate (DAKO Japan) or HistoGreen/HISTOPRIME® (E109; Linaris-Biologische Produkte) was used for the development of IHC. For quantification of HE and IHC, 7 week old PKF mice ($n = 7$) and PKF2h mice ($n = 6$) were consecutively analyzed by the investigator blinded to the group allocation. Four random files from each sample were analyzed at 200 \times original magnification and positive cells were counted in the tumor ductal lumen, juxtatumoral, or dense interlobular stroma with desmoplastic reaction (desmoplastic stroma).

Statistics

All data of in vitro are indicated as means \pm standard error (SE), while in vivo data are indicated as means \pm standard deviation. Statcel software version 4 (OMS Ltd.) and JMP statistical software (SAS Institute, Inc.) were used for the statistical calculations³⁶. Two-sided student's *t* test was used for the in vitro invasion/migration, proliferation and qRT-PCR analyses. Two-sided Mann–Whitney's *U* test was used to determine the significant difference in histopathological analyses. For

comparison of survival in Kaplan–Meier analyses, littermates of PKF ($n = 27$) and PKF2h ($n = 25$) were consecutively employed and log-rank test was used for univariate survival analyses. $P < 0.05$ was the threshold for statistical significance.

Acknowledgments

We thank Christopher VE Wright (Vanderbilt University) for *Ptfla*^{cre/+} mice, Tyler Jacks (Massachusetts Institute of Technology) for *LSL-Kras*^{G12D/+} mice, Mitsuko Tsubouchi (The University of Tokyo) for technical assistance, and laboratory members for helpful discussions. This work was supported by the Japanese Society for the Promotion of Science Kakenhi Grant 25430106 and 16K07109, and the Nakayama Cancer Research Institute.

Authors' contributions

M.S. and H.I. designed experiments, acquired and analyzed data, and wrote the manuscript. H.F. and Y.M. also acquired data. R.T., K.M., T.Y., H.K., T.N., Y.T., and K. T. discussed data. H.L.M. reviewed the manuscript. H.I. and K.K. supervised the study.

Author details

¹Department of Gastroenterology, Graduate School of Medicine, The University of Tokyo, 7-3-1 Hongo, Bunkyo-ku, Tokyo 113-8655, Japan. ²Division of Human Pathology, Department of Pathology and Microbiology, Nihon University School of Medicine, 30-1 Oyaguchikamicho, Itabashi-ku, Tokyo 173-8610, Japan. ³Department of Clinical Nutrition Therapy, Graduate School of Medicine, The University of Tokyo, 7-3-1 Hongo, Bunkyo-ku, Tokyo 113-8655, Japan. ⁴Department of Molecular Pathology, Graduate School of Medicine, The University of Tokyo, 7-3-1 Hongo, Bunkyo-ku, Tokyo 113-0033, Japan. ⁵Vanderbilt-Ingram Comprehensive Cancer Center, Vanderbilt University, 691 Preston Building, Nashville, TN 37232, USA. ⁶Department of Gastroenterology, Juntendo University School of Medicine, 3-1-3 Hongo, Bunkyo-ku, Tokyo 113-8431, Japan

Conflict of interest

The authors declare that they have no conflict of interest.

Publisher's note

Springer Nature remains neutral with regard to jurisdictional claims in published maps and institutional affiliations.

Supplementary Information accompanies this paper at (<https://doi.org/10.1038/s41389-018-0117-8>).

Received: 4 September 2018 Revised: 23 November 2018 Accepted: 20 December 2018

Published online: 18 January 2019

References

1. Siegel, R. L., Miller, K. D. & Jemal, A. Cancer Statistics, 2017. *CA Cancer J. Clin.* **67**, 7–30 (2017).
2. Kato, K. Vital Statistics in Japan. Director-General for statistics and Information Policy, Ministry of Health, Labour and Welfare, Tokyo, pp. 18–19 (2017).
3. Warshaw, A. L. & Fernandez-del Castillo, C. Pancreatic carcinoma. *N. Engl. J. Med.* **326**, 455–465 (1992).
4. Bardeesy, N. & DePinho, R. A. Pancreatic cancer biology and genetics. *Nat. Rev. Cancer* **2**, 897–909 (2002).
5. Hruban, R. H. et al. Pancreatic intraepithelial neoplasia: a new nomenclature and classification system for pancreatic duct lesions. *Am. J. Surg. Pathol.* **25**, 579–586 (2001).
6. Rozenblum, E. et al. Tumor-suppressive pathways in pancreatic carcinoma. *Cancer Res.* **57**, 1731–1734 (1997).
7. Jones, S. et al. Core signaling pathways in human pancreatic cancers revealed by global genomic analyses. *Science* **321**, 1801–1806 (2008).

8. Wagner, M., Kleeff, J., Friess, H., Buchler, M. W. & Korc, M. Enhanced expression of the type II transforming growth factor-beta receptor is associated with decreased survival in human pancreatic cancer. *Pancreas* **19**, 370–376 (1999).
9. Venkatasubbarao, K. et al. Differential expression of transforming growth factor beta receptors in human pancreatic adenocarcinoma. *Anticancer Res.* **20**, 43–51 (2000).
10. Ijichi, H. et al. Aggressive pancreatic ductal adenocarcinoma in mice caused by pancreas-specific blockade of transforming growth factor-beta signaling in cooperation with active Kras expression. *Genes Dev.* **20**, 3147–3160 (2006).
11. Ijichi, H. et al. Inhibiting Cxcr2 disrupts tumor-stromal interactions and improves survival in a mouse model of pancreatic ductal adenocarcinoma. *J. Clin. Invest.* **121**, 4106–4117 (2011).
12. Belperio, J. A. et al. Critical role for CXCR2 and CXCR2 ligands during the pathogenesis of ventilator-induced lung injury. *J. Clin. Invest.* **110**, 1703–1716 (2002).
13. Del Rio, L., Bennouna, S., Salinas, J. & Denkers, E. Y. CXCR2 deficiency confers impaired neutrophil recruitment and increased susceptibility during *Toxoplasma gondii* infection. *J. Immunol.* **167**, 6503–6509 (2001).
14. Mehrad, B. et al. CXC chemokine receptor-2 ligands are necessary components of neutrophil-mediated host defense in invasive pulmonary aspergillosis. *J. Immunol.* **163**, 6086–6094 (1999).
15. Sue, R. D. et al. CXCR2 is critical to hyperoxia-induced lung injury. *J. Immunol.* **172**, 3860–3868 (2004).
16. Strieter, R. M. et al. Cancer CXC chemokine networks and tumour angiogenesis. *Eur. J. Cancer* **42**, 768–778 (2006).
17. Vandercappellen, J., Van Damme, J. & Struyf, S. The role of CXC chemokines and their receptors in cancer. *Cancer Lett.* **267**, 226–244 (2008).
18. Steele, C. W. et al. CXCR2 inhibition profoundly suppresses metastases and augments immunotherapy in pancreatic ductal adenocarcinoma. *Cancer Cell.* **29**, 832–845 (2016).
19. Matsuo, Y. et al. CXC-chemokine/CXCR2 biological axis promotes angiogenesis in vitro and in vivo in pancreatic cancer. *Int. J. Cancer* **125**, 1027–1037 (2009).
20. Strieter, R. M. et al. The functional role of the ELR motif in CXC chemokine-mediated angiogenesis. *J. Biol. Chem.* **270**, 27348–27357 (1995).
21. Devalaraja, R. M. et al. Delayed wound healing in CXCR2 knockout mice. *J. Invest. Dermatol.* **115**, 234–244 (2000).
22. Dyer, D. P. et al. CXCR2 deficient mice display macrophage-dependent exaggerated acute inflammatory responses. *Sci. Rep.* **7**, 42681 (2017).
23. Youn, J. I. & Gabrilovich, D. I. The biology of myeloid-derived suppressor cells: the blessing and the curse of morphological and functional heterogeneity. *Eur. J. Immunol.* **40**, 2969–2975 (2010).
24. Mills, C. D. M1 and M2 macrophages: oracles of health and disease. *Crit. Rev. Immunol.* **32**, 463–488 (2012).
25. Zheng, X. et al. Redirecting tumor-associated macrophages to become tumoricidal effectors as a novel strategy for cancer therapy. *Oncotarget* **8**, 48436–48452 (2017).
26. Matsuo, Y. et al. K-Ras promotes angiogenesis mediated by immortalized human pancreatic epithelial cells through mitogen-activated protein kinase signaling pathways. *Mol. Cancer Res.* **7**, 799–808 (2009).
27. Xu, Z. et al. Role of pancreatic stellate cells in pancreatic cancer metastasis. *Am. J. Pathol.* **177**, 2585–2596 (2010).
28. Liou, G. Y. et al. Macrophage-secreted cytokines drive pancreatic acinar-to-ductal metaplasia through NF-kappaB and MMPs. *J. Cell Biol.* **202**, 563–577 (2013).
29. Pollard, J. W. Tumour-educated macrophages promote tumour progression and metastasis. *Nat. Rev. Cancer* **4**, 71–78 (2004).
30. Sica, A. & Mantovani, A. Macrophage plasticity and polarization: in vivo veritas. *J. Clin. Invest.* **122**, 787–795 (2012).
31. Zheng, X. F. et al. Lipopolysaccharide-induced M2 to M1 macrophage transformation for IL-12p70 production is blocked by *Candida albicans* mediated up-regulation of EB13 expression. *PLoS One* **8**, e63967 (2013).
32. Yamamoto, K. et al. Stromal remodeling by the BET bromodomain inhibitor JQ1 suppresses the progression of human pancreatic cancer. *Oncotarget* **7**, 61469–61484 (2016).
33. Tanaka, Y. et al. Sharpin promotes hepatocellular carcinoma progression via transactivation of Versican expression. *Oncogenesis* **5**, e277 (2016).
34. Keane, M. P., Belperio, J. A., Xue, Y. Y., Burdick, M. D. & Strieter, R. M. Depletion of CXCR2 inhibits tumor growth and angiogenesis in a murine model of lung cancer. *J. Immunol.* **172**, 2853–2860 (2004).
35. Sano, M. et al. Activation of WNT/beta-catenin signaling enhances pancreatic cancer development and the malignant potential via up-regulation of Cyr61. *Neoplasia* **18**, 785–794 (2016).
36. Sano, M. et al. Induction of cell death in pancreatic ductal adenocarcinoma by indirubin 3'-oxime and 5-methoxyindirubin 3'-oxime in vitro and in vivo. *Cancer Lett.* **397**, 72–82 (2017).